Hydrobiologia (2022) 849:3041–3059
https://doi.org/10.1007/s10750-022-04912-x

PRIMARY RESEARCH PAPER

Impact of Post-Tropical Storm Arthur (2014) on benthic Arcellinida assemblage dynamics in Harvey Lake, New Brunswick, Canada

Dan Atasiei · Nawaf A. Nasser · Calder W. Patterson · Anqi Wen · R. Timothy Patterson · Jennifer M. Galloway · Helen M. Roe

Received: 3 November 2021 / Revised: 24 March 2022 / Accepted: 16 May 2022 / Published online: 15 June 2022

Abstract Arcellinida (testate lobose amoebae) were examined in surface-sediment samples collected in 2015 from throughout Harvey Lake, New Brunswick, Canada to assess whether the passage of Post-Tropical Storm Arthur in 2014 impacted the distribution of taxa and assemblages. Cluster analysis and non-metric multidimensional scaling (NMDS) revealed four distinct arcellinidan assemblages: (1) Deep Water Reworking Assemblage (DWR; approximately unbiased, AU *P*-value = 89%); (2) Arsenic Impact Assemblage (AI; AU *P*-value = 92%); (3) Northern Shallow Water Assemblage A (NSWA; AU *P*-value = 66%); and (4) Northern Shallow Water Assemblage B (NSWB; AU *P*-value = 0%). Redundancy analysis (RDA) and partial-RDA results were used to identify four variables that significantly influenced the assemblage composition and explained 20.2% of the arcellinidan distributional variability: [arsenic (As), wind mixing probability (WMP), water depth and sedimentary grain size represented by the very coarse silt end member 2 (EM2) which was 40 µm]. Arsenic concentration in the sediments of Harvey Lake is an important control over the distribution of Arcellinida assemblages. Levels of sedimentary As in samples from the southern part of Harvey Lake, near As-bearing volcanic bedrock in the catchment, exceeded the Probable Effect Level (17 ppm) and Interim Sediment Quality Guideline (5.9 ppm) for this element. Shallower water (less than median water depth of 3.56 m) and highly diverse assemblages NSWA and NSWB (median SDI = 2.6) significantly correlated with wind mixing probability, while deeper water (greater than median = 6.2 m) and moderately to highly diverse assemblages DWR and AI (SDI range 2.4–2.7) associated strongly with EM2. EM2 was derived from the suspension of and redeposition of sediments when the storm water wave base was deepened during the passage of Arthur. Arcellinidans were carried into suspension along with very coarse silt grain particles

Handling Editor: Jasmine Saros

Supplementary Information The online version contains supplementary material available at https://doi.org/10.1007/s10750-022-04912-x.

D. Atasiei (✉) · N. A. Nasser · A. Wen · R. T. Patterson · J. M. Galloway
Ottawa-Carleton Geoscience Centre and Department of Earth Sciences, Carleton University, 1125 Colonel by Drive, Ottawa, ON K1S 5B6, Canada
e-mail: danatasiei13@gmail.com

C. W. Patterson
Department of Geography and Environmental Studies, Carleton University, 1125 Colonel by Drive, Ottawa K1S 5B6, Canada

J. M. Galloway
Geological Survey of Canada (GSC)/Commission géologique du Canada, Natural Resources Canada (NRCan)/Ressources naturelles Canada (RNCan), 3303-33 Street N.W., Calgary, AB T2L 2A7, Canada

H. M. Roe
School of Natural and Built Environment, Queen's University Belfast, Belfast BT71NN, UK

during the passage of the storm and redeposited at all water depths when wave energy decreased. Water depth of sampling stations should be taken into consideration in lakes that may be periodically impacted by large storms.

Keywords Testate lobose amoebae · Intra-lake sampling · Assemblage dynamics · Storm wave base · Wind mixing probability · Multivariate analysis

Introduction

Major tropical storms and hurricanes are among the most devastating natural hazards, annually causing severe socio-economic and ecological impacts across the world (Pachauri et al., 2014). There is a growing concern that future storm and hurricane events may become more abrupt, intense, and frequent because of climate warming (Mitchell et al., 1990; Haarsma et al., 1993; Alley et al., 2003; Webster et al., 2005; Pachauri et al., 2014). In addition, storms and hurricanes are expected to extend their geographical region of impact, reaching beyond coastal sedimentary environments to terrestrial aquatic systems, including inland lakes (Eden and Page, 1998; Alley et al., 2003; Webster et al., 2005; Pachauri et al., 2014). A small, yet growing, number of studies have demonstrated the significant impact that major storms and hurricanes can have on lacustrine environments (e.g., Eden and Page, 1998; Patterson et al., 2020).

Major storms, and especially hurricanes, are often associated with substantial precipitation and intense winds that can have several effects on lacustrine sedimentation (Oliva et al., 2018). For instance, storm-induced precipitation often enhances the erosion and transportation of sediment from the surrounding catchment to lakes via surface runoff (Jensen et al., 2012; Gallagher et al., 2016; Oliva et al., 2018; Patterson et al., 2020), while intense storm winds trigger remobilization of lake sediments through deepening the storm wave base (Peng et al., 2005; Patterson et al., 2020).

A recent example of the impact of major storm-driven sediment resuspension was documented in Harvey Lake (45° 43′ 45″ N, 67° 00′ 25″ W), New Brunswick, Canada related to the passage of Post-Tropical Storm Arthur in July 2014. Winds associated with Arthur generated large waves that remobilized a considerable amount of lake bottom sediment in areas where water depth was shallower than 4.4 m water depth (maximum theoretical storm wave base depth) into the overlaying water column (Patterson et al., 2020). The counterclockwise wind field of the storm pushed these suspended sediments toward the southwestern section of Harvey Lake, where they were redeposited at all water depths. While that study focused on assessing the direct impact of the storm on Harvey Lake bottom sedimentation, the storm undoubtedly impacted other lacustrine geochemical and biological proxies as well. In particular, biological proxies (i.e., bioindicators) are highly valued in lacustrine studies, with benthic microorganisms, like Arcellinida (testate lobose amoebae), being among the most commonly employed bioindicators due to their sensitivity to a wide range of changes in lacustrine environmental conditions (e.g., Patterson and Kumar, 2002; Nasser et al., 2016, 2020a).

Arcellinida are a group of benthic shelled protists found worldwide that live in a wide array of freshwater environments (e.g., lakes, rivers, and peatlands; Ogden and Hedley, 1980; Medioli and Scott, 1983; Patterson et al., 1985) and, to a lesser extent, brackish habitats (Patterson et al., 1985; Charman et al., 2000). The living organism resides within a test (i.e., shell) that is either secreted by the organism (i.e., autogenous) or formed by agglutinating materials like diatoms frustules or sand particles (i.e., xenogenous; Medioli and Scott, 1983). During the past several years there has been a growing focus on exploring the use of Arcellinida as indicators of environmental variability in limnological and paleolimnological studies; particularly geostatistical analysis to better understand relationships between the distribution of taxa and environmental variables (e.g., Kihlman and Kauppila, 2012; Nasser et al., 2016, 2020a; Riou et al., 2021). A major advantage of using this group lies in their great abundance in organic-rich sediments, rapid reproduction rate (days to weeks), resistivity of their tests to decay, relative ease of taxonomic identification, and their sensitivity to change in a plethora of environmental variables (e.g., pH, water temperature, water quality, salinity, eutrophication, land-use, and pollutants; Patterson and Kumar, 2002; Nasser et al., 2015). These traits render Arcellinida useful for performing spatio-temporal limnological assessments (Patterson & Kumar, 2002; Nasser et al., 2016). While the impact of paleo-storm and hurricane

events on other microbial groups has been examined (e.g., diatoms and foraminifera; Miller et al., 1988; Engle et al., 2009; Pilarczyk et al., 2014), the impact of such events on the spatial distribution of lacustrine Arcellinida assemblages in freshwater environments has yet not been assessed. Because Arcellinida are used to reconstruct past limnological and climate conditions, understanding of the impact of storms on their distribution in surficial lake sediments is needed in areas affected by extreme weather events.

In this study, Arcellinida were examined from 33 surface-sediment samples collected from Harvey Lake in 2015, the year following the passage of Post-Tropical Storm Arthur, to assess the impact of storm derived deepening of the wave base on the intra-lake distribution of Arcellinida. The authors hypothesize that distinct Arcellinida assemblages will be identified above and below the wave base depth associated with Hurricane Arthur. Harvey Lake was an ideal place to carry out this research as a recent study by Patterson et al. (2020) already demonstrated that the lake bottom substrate was indeed impacted by Arthur in 2014 with a water depth of 4.4 m being identified as the maximum storm wave base for that event. The 33 surface-sediment samples analyzed for this study are a subset of the 100 surface-sediment samples used in the Patterson et al. (2020; details pertaining to analysis performed on the samples are presented in the paper).

Study area

Harvey Lake (45° 43′ 38″ N, 67° 00′ 59″ W) is located near the village of Harvey, York County, New Brunswick, Canada (Fig. 1A). The lake is situated in the eastern Canada temperate climate zone, with an average annual precipitation and temperature of 19 cm and ~ 5.1°C, respectively (Bailey et al., 1997). Harvey Lake has a relatively small surface area (7.15 km^2) and a maximum depth of 11.8 m (Fig. 1B). There are two relatively small inlet streams flowing into the Harvey Lake: Sucker Brook entering at the head of Herbert's Cove at the southwest corner of the lake,

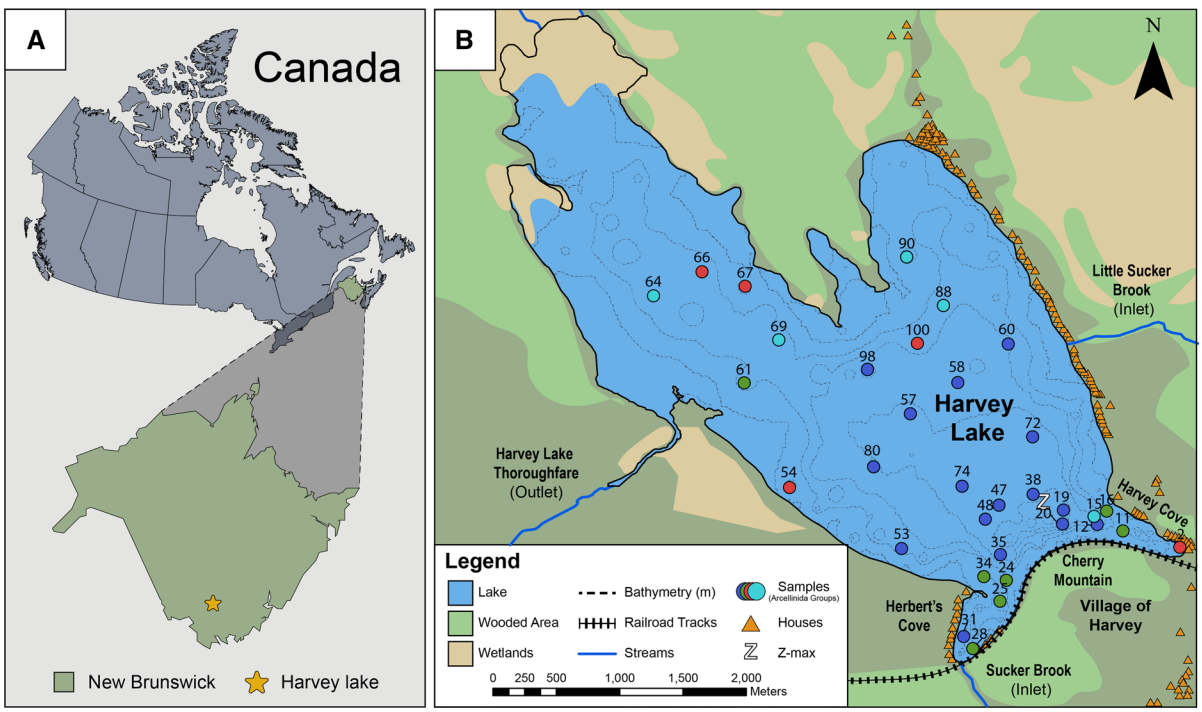

Fig. 1 Map of the study area. A map of Canada showing the study area in New Brunswick, Canada (represented by the yellow star). **B** A map showing Harvey Lake and the location of the sampling stations for the 33 samples containing statistically significant populations of Arcellinida. The colored circles represent the four identified Arcellinida assemblages

and Little Sucker Brook flowing into the lake midway along the eastern margin of the lake (Fig. 1B). A single outlet stream, "The Harvey Lake Thoroughfare", flows out of the lake midway along the western shore and into the Second Harvey Lake (also known as Mud Lake). There are ~ 160 homes and cottages concentrated in the Herbert's Cove area and along the route of Highway 636 on the eastern margin of the lake, with agricultural land positioned behind them. Between Harvey Lake and Second Harvey Lake, there are extensive areas of wetland. Cherry Mountain with a maximum elevation of 240 m is located at the south end of the lake (Fig. 1B). It is comprised of Late Devonian and Early Carboniferous Harvey Group rocks of the Harvey Mountain and Cherry Hill formations (Pajari & Rast, 1973). The 100 m thick exposure of the Cherry Hill Formation consists of quartz–feldspar phyric densely welded ash-flow tuff ("quartz/feldspar porphyry"), with poorly welded ash flow sheets at the base. It also consists other ignimbrites and volcaniclastic sedimentary rocks. The 75 to 100 m thick sequence comprising the Harvey Mountain Formation is characterized by laminated rhyolite lava flows, pyroclastic breccia, and ignimbrites intercalated with ash-fall tuffs (Dostál et al., 2016). Sucker Brook flows through forest over outcrops of both the Cherry Hill and Harvey Mountain formations, while Little Sucker Brook flows through agricultural land to the east of the lake over Silurian metasedimentary basement rocks (McKerrow and Ziegler, 1971).

Materials and methods

Sampling design and field methods

A total of 100 sediment–water interface samples were collected from Harvey Lake during summer of 2015, which as described above were used to assess the impact of Post-Tropical Storm Arthur on lake bottom sedimentation (Patterson et al., 2020; Fig. 1B). Sampling sites were distributed throughout the lake to ensure a maximum spatial coverage. Sample collection was carried out using the Ekman grab sampler with the top 0.5 cm of each grab being collected for various analyses. From these 100 surface-sediment samples, an initial subset of 37 surface-sediment samples were randomly selected using a Google random number generator for the micropaleontological arcellinidan analysis carried out here. Water depth was measured with SONAR and it was verified by depth indicators (marks on the rope) on the Ekman grabber.

Laboratory methods

Geochemical analysis

All 37 selected surface-sediment samples were previously analyzed using relative counts per second Itrax core-scanning X-ray fluorescence (XRF-CS) XRF calibrated to quantitative ICP-MS values (Gregory et al., 2019) using the multivariate log ratio calibration methodology of Weltje et al. (2015). Using this calibration technique, the Itrax-XRF results were then converted from counts per second to parts per million (ppm) for aluminum oxide; arsenic; calcium oxide; iron(III) oxide; potassium oxide; manganese(II) oxide; lead; titanium(IV) oxide; and, zirconium. The calibrated values were used as variables in the present study.

Particle size analysis

The 37 surface-sediment samples were analyzed for particle size analysis using a method modified from Murray (2002) and van Hengstum et al. (2007). Surface-sediment samples were treated with HCl (10%) and H_2O_2 (30%) to remove carbonates and organic matter, respectively. Treated surface-sediment sample were incubated in a 70°C water bath to speed up the digestion process. A Beckman Coulter LS 13 320 laser diffraction particle size analyzer (0.3 to 2,000 µm range) was then used to analyze the treated subsamples. To load the instrument, suspended subsamples were added until an obscuration of $10 \pm 3\%$ was met. Three replicates were analyzed for each subsample, and their average was recorded as the particle size distribution.

Arcellinidan analysis

A 1 cubic centimeter (cm^3) subsample was obtained from each sample using a modified syringe. The one cc subsample volume had statistically significant numbers of arcellinidan specimens. Subsamples were then wet sieved using a 297 µm and 37 µm sieves to, respectively, remove large organic debris and to

capture the arcellinidan tests. The sieved subsamples were then gently washed under running water for two minutes to further eliminate fine debris (< 37 µm) and remaining organic matter. Subsamples were then divided into six splits using a wet sample splitter to improve counting efficiency by further reducing organic matter concentration (Scott and Hermelin, 1993). Sample splits were counted using an Olympus SZH dissecting binocular microscope (×7.5–64 magnification) until statistically significant total counts were obtained for each surface-sediment sample (170–200 tests; Patterson and Fishbein, 1989). Species and strains of arcellinidan were identified using key well-illustrated publications that employed the strain concept (e.g., Reinhardt et al., 1998a, b; Roe et al., 2010; Patterson et al., 2013; Nasser et al., 2016) as well as the Microworld online database (Siemensma, 2019). The count results were tabulated and then converted into relative species abundance using the decostand function of the vegan package in the R statistical language through R Studio (version 0.98.1028; R Core Team, 2014; Appendix 2—Supplementary Material).

Statistical analysis

Data screening

Of the 37 subsamples, 4 (1, 5, 86, and 92) were barren for Arcellinida and therefore removed from subsequent analysis. Twenty-five Arcellinida species and strains were identified in the 33 sub-samples (Appendix 2—Supplementary Material). The probable error (pe) was calculated for each sub-sample in R Studio based on the following equation:

$$\mathrm{pe} = 1.96\left(\frac{S}{\sqrt{\mathrm{Xi}}}\right),$$

where S is the standard deviation of the population count and Xi is the fractional abundance (Patterson & Fishbein, 1989). A sample count was deemed statistically insignificant if the probable error exceeded the total count for a sample. All surface-sediment samples contained statistically significant populations. Standard error (Sxi) was calculated for the identified Arcellinida species in R Studio based on the following equation:

$$\mathrm{Sxi} = 1.96\sqrt{\frac{F1(1-F1)}{\mathrm{Ni}}},$$

where $F1$ is the fractional abundance of species and Ni is the total number of counts. Species were considered to be present in statistically insignificant numbers if the standard error exceeded the total counts for that species in all sub-samples (Patterson & Fishbein, 1989). Based on this analysis eight species or strains were removed from further consideration; *Arcella vulgaris* Ehrenberg 1830, *Centropyxis constricta* (Ehrenberg 1843) strain "constricta," *Cucurbitella tricuspis* (Carter 1856), *Mediolus corona* (Wallich 1864), *Difflugia fragosa* Hemple 1902, *Difflugia glans* Penard 1902 strain "distenda," and *Difflugia nodosa* (Leidy 1879). *Cucurbitella tricuspis* was also removed from the data set because this taxon has a planktic phase resulting in it becoming distributed by currents and waves throughout the lake basin into lake environments where it did not necessarily live. The Shannon diversity index (SDI; Shannon, 1948) was calculated using the diversity function of the vegan package in R Studio (version 0.98.1028; R Core Team, 2014) to assess arcellinidan diversity as a measure of ecological health. Identified arcellinidan assemblages were considered healthy if the SDI was > 2.5, in transition if SDI was between 1.5 and 2.5, and stressed if SDI was < 1.5 (Magurran, 1988; Patterson & Kumar, 2002).

Spearman rank correlation

Spearman rank correlation was performed using the cor function (Taiyum & Wei, 2016) of the stats package in R Studio to examine interesting associations between Arcellinida species and the parameters and to reduce collinearity in the analyzed data sets. The Arcellinida and measured parameters data sets were combined in a single Excel spreadsheet to test for correlation probabilities between each variable within a 95% confidence interval. A P-value was calculated for each pair of variable combination to represent the statistical significance of their correlation. Variable pairs with P-values less than 0.05 were considered to have a statistically significant relationship. A correlogram was generated, using the corrplot function of the package corrplot in R Studio, to visualize correlations between each pair of variables (Fig. 2).

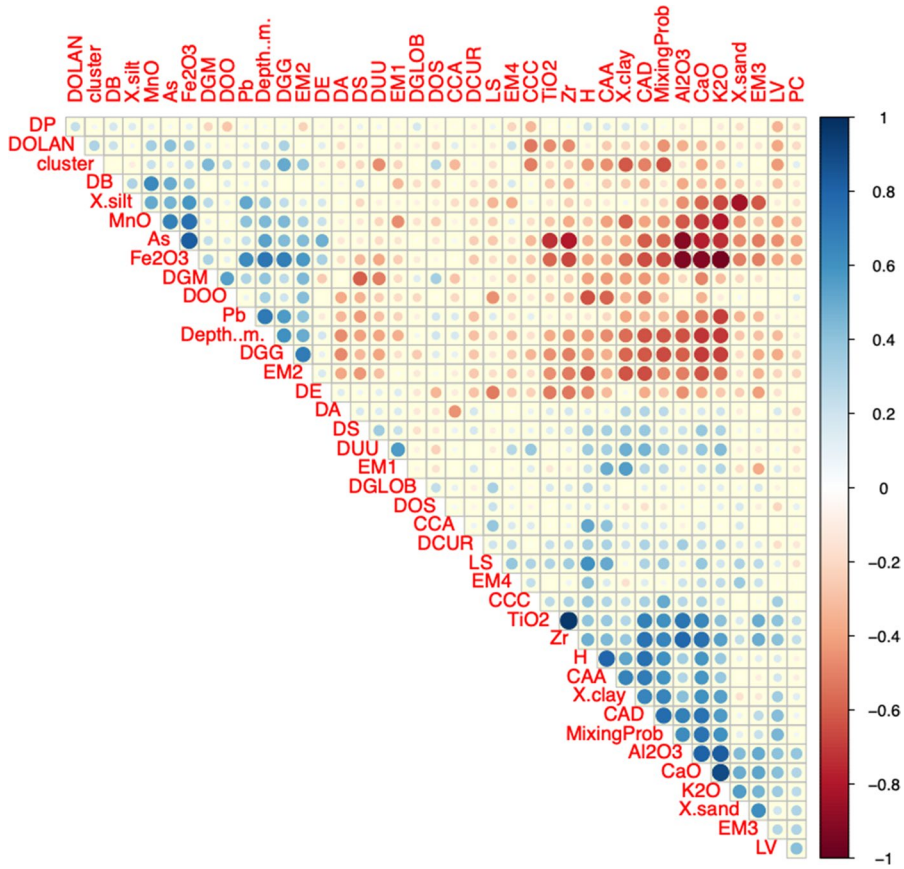

Fig. 2 Spearman rank correlation correlogram. The strength of the correlation between any pair is represented by the size and color of the circle. The bigger the circle, the stronger the correlation. Blue circles represent positive relationships, while red circles represent negative correlations. The darker the color the greater the relationship and vice versa

Cluster analysis

Hierarchical Q- and R-modes cluster analysis was performed on vetted relative arcellinidan abundance data using the hclust function of the stats package in R Studio to identify patterns in the Arcellinida data set. Q-mode was used to define groups containing surface-sediment samples with similar assemblage structures (Appendix 3—Supplementary Material), while R-mode identified the statistical relationships between arcellinidan species and strains. The results of Q- and R-modes were further supported by the PVClust procedure, which was used to identify the level of statistical significance for the identified arcellinidan assemblages. This was performed using the PVClust function and package in R Studio (Suzuki & Shimodaira, 2006). The relative abundance data was first normalized using Hellinger transformation (Rao, 1995). Hellinger transformation was chosen as it minimized problems that often occur when using community data, which is critical for subsequent multivariate analysis (e.g., redundancy analysis, RDA; Legendre and Gallagher, 2001). The Euclidean distances between each surface-sediment sample and each species were calculated, then analyzed using Ward's minimum variance clustering method (Ward, 1963; Fishbein and Patterson, 1993). Ward's minimum variance clustering method was chosen for cluster analysis as it produced superior and well-structured dendrograms compared to other hierarchical clustering methods (e.g., single-, complete-, and average-linkage hierarchical clustering). Finally, a dendrogram and heat map was produced to illustrate possible arcellinidan groups using the pheatmap function of the package pheatmap (Maintainer & Kolde, 2019) in R Studio (Fig. 3).

Non-metric multidimensional scaling

Non-metric multidimensional scaling (NMDS; Kruskal, 1964) was used to evaluate the residual Arcellinida data set ($n = 33$ surface-sediment

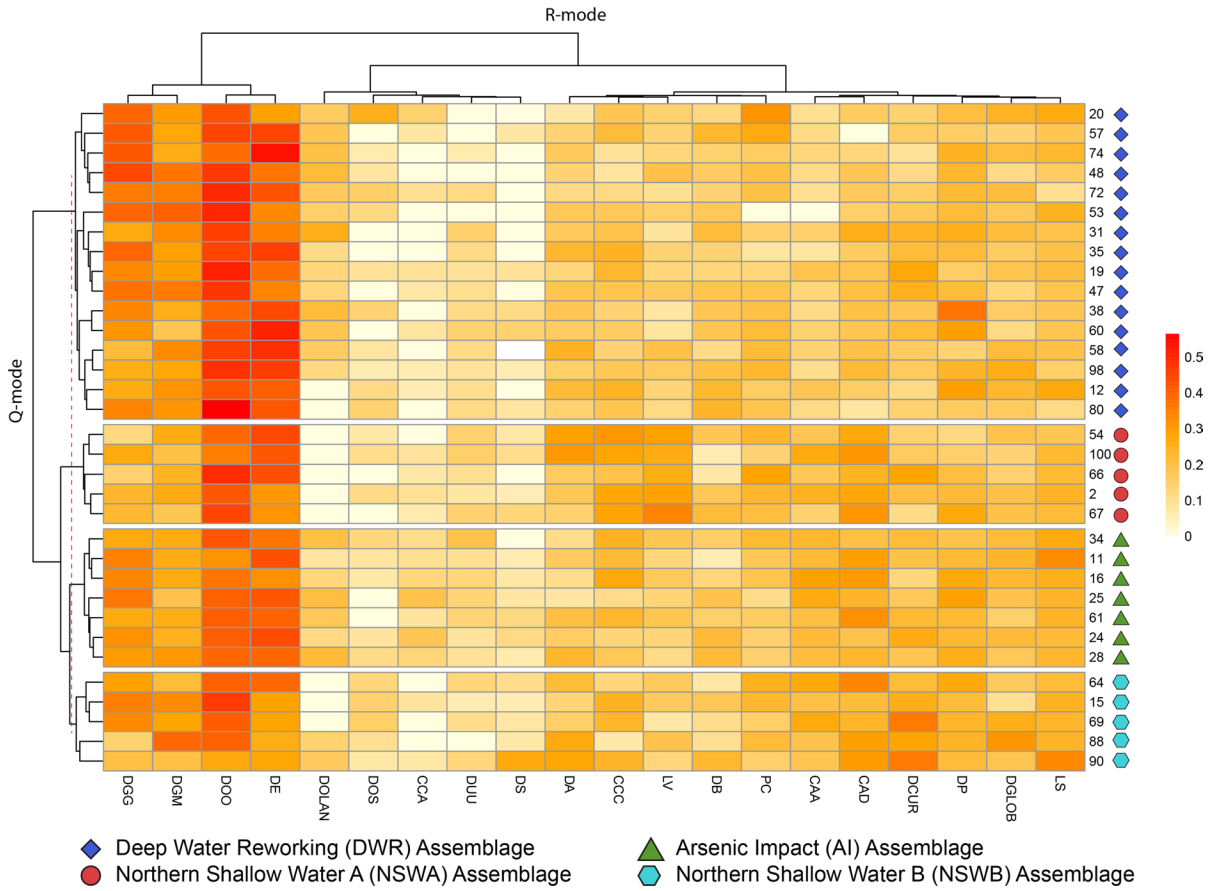

Fig. 3 Arcellinida assemblages relying on a two-way heatmap cluster analysis. The heatmap shows the relative abundance of 20 identified Arcellinida species and strains (R-mode; horizontal dendrogram) in the samples of the identified assemblages (Q-mode; vertical dendrogram). The colored numbers show the results of the PVClust analysis. The red number shows the statistical significance of the identified numbers. The different assemblages are on the left-hand side. *CAA Centropyxis aculeata* "aculeata," *CAD Centropyxis aculeata* "discoides," *CCA Centropyxis constricta* "aerophila," *CCC Centropyxis constricta* "constricta," *DB Difflugia bidens*, *DGG Difflugia glans* "glans," *DGM Difflugia glans* "magna," *DOLAN Difflugia oblonga* "lanceolata," *DOO Difflugia oblonga* "oblonga," *DOS Difflugia oblonga* "spinosa," *DA Difflugia acuminata*, *DE Difflugia elegans*, *DP Difflugia protaeiformis*, *DS Difflugia scalpellum*, *DGLOB Difflugia globulosa*, *DCUR Difflugia curvicaulis*, *DUU Difflugia urceolata* "urceolata," *PC Pontigulasia compressa*, *LS Lesquereusia spiralis*, *LV Lagenodifflugia vas*

samples) to examine the relationships between the Arcellinida species and surface-sediment samples in a reduced multidimensional space. This methodology plots similar groups together and dissimilar ones away from each other using the Bray–Curtis dissimilarity matrix. The grouping of similar data points can then be interpreted from a two-dimensional ordination graph (i.e., biplot). Therefore, NMDS was also used to confirm, or refute, the results of hierarchical clustering (Fig. 4).

Redundancy analysis

RDA was performed to quantify the relationship between the measured parameters and the identified arcellinidan assemblages. Specifically, 33 variables and 20 Arcellinida species were considered to derive the preliminary RDA model (Appendices 1, 2—Supplementary Material). The species (Hellinger transformation) and measured parameters data sets (scaled and log-transformed) were transformed to satisfy the

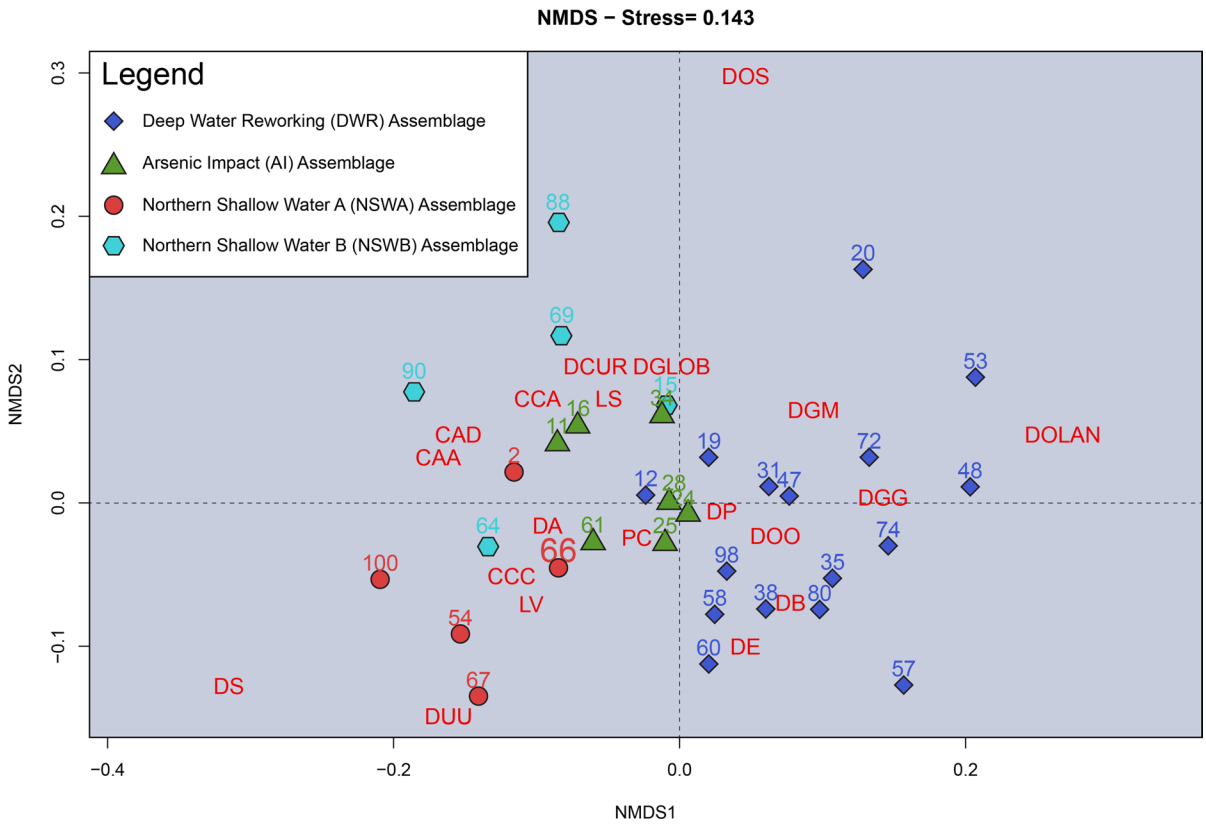

Fig. 4 Nonmetric multidimensional scaling (NMDS) bi-plot. The colored symbols represent the four Arcellinida Assemblages. The red acronyms represent the statistically significant Arcellinida taxa. The stress value is 0.143. *CAA Centropyxis aculeata* "aculeata," *CAD Centropyxis aculeata* "discoides," *CCA Centropyxis constricta* "aerophila," *CCC Centropyxis constricta* "constricta," *DB Difflugia bidens*, *DGG Difflugia glans* "glans," *DGM Difflugia glans* "magna," *DOLAN Difflugia oblonga* "lanceolata," *DOO Difflugia oblonga* "oblonga," *DOS Difflugia oblonga* "spinosa," *DA Difflugia acuminata*, *DE Difflugia elegans*, *DP Difflugia protaeiformis*, *DS Difflugia scalpellum*, *DGLOB Difflugia globulosa*, *DCUR Difflugia curvicaulis*, *DUU Difflugia urceolata* "urceolata," *PC Pontigulasia compressa*, *LS Lesquereusia spiralis*, *LV Lagenodifflugia vas*

RDA assumptions (Legendre and Gallagher, 2001). Following the initial analysis, four statistically significant variables [end member 2 (EM2), wind mixing probability (WMP), water depth, and arsenic] as described in detail below were selected for the final RDA model. Partial-RDA and variance partitioning were performed on the selected variables to determine the amount of variance in Arcellinida distribution explained by each variable (Fig. 5).

End member mixing analysis (EMMA)

EMMA is a method used to provide an interpretation of multi-modal grain size distributions while minimizing assumptions (Weltje & Prins, 2003, 2007; Dietze et al., 2012). End members (EMs) are modeled by un-mixing multi-modal distributions that are comprised of the sum of many depositional processes, and the resultant EMs can then be associated with specific depositional processes (Macumber et al., 2018). A detailed description of the EMMA procedure used to derive EM2 used here is provided by Patterson et al. (2020). In their EMMA analysis of the Harvey Lake sediment distribution, Patterson et al. (2020) determined that EM2 was deposited as a result of the passage of Post-Tropical Storm Arthur, and for this reason was included in the RDA analysis.

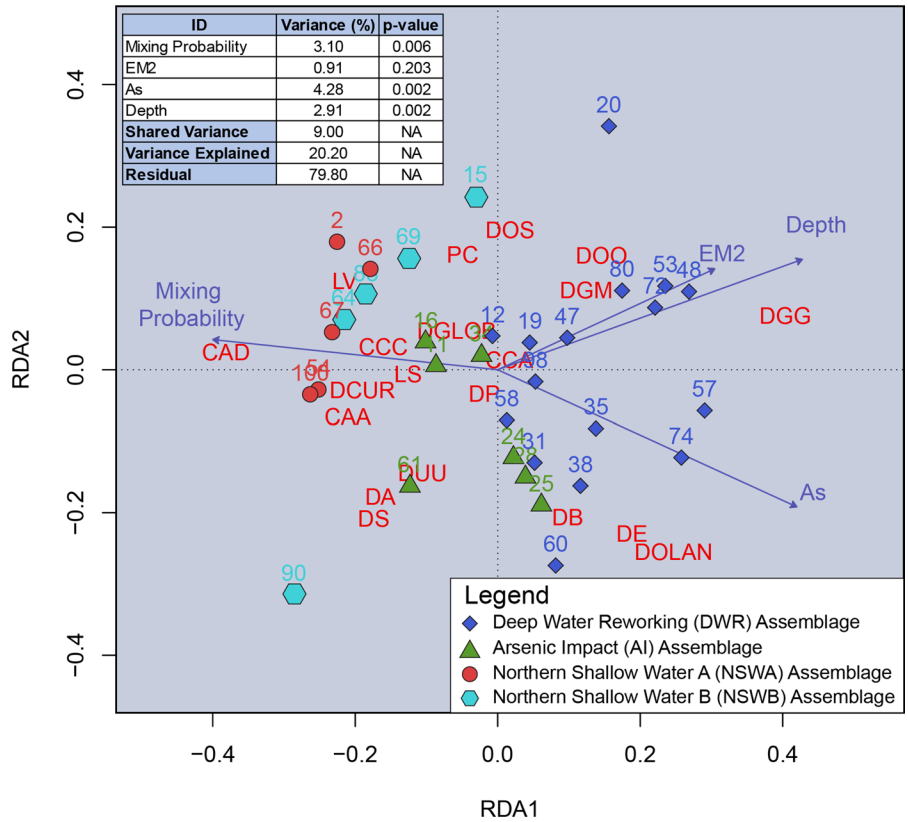

Fig. 5 Redundancy analysis (RDA) and variance partitioning results. RDA triplot for the Harvey Lake datasets. Variance partitioning is in top left corner. The colored symbols represent the four identified Arcellinida Assemblages. The red acronyms represent the statistically significant Arcellinida taxa. The arrows represent the different parameters selected for the RDA model. The partial-RDA results are in the top left corner. *CAA Centropyxis aculeata* "aculeata," *CAD Centropyxis aculeata* "discoides," *CCA Centropyxis constricta* "aerophila," *CCC Centropyxis constricta* "constricta," *DB Difflugia bidens*, *DGG Difflugia glans* "glans," *DGM Difflugia glans* "magna," *DOLAN Difflugia oblonga* "lanceolata," *DOO Difflugia oblonga* "oblonga," *DOS Difflugia oblonga* "spinosa," *DA Difflugia acuminata*, *DE Difflugia elegans*, *DP Difflugia protaeiformis*, *DS Difflugia scalpellum*, *DGLOB Difflugia globulosa*, *DCUR Difflugia curvicaulis*, *DUU Difflugia urceolata* "urceolata," *PC Pontigulasia compressa*, *LS Lesquereusia spiralis*, *LV Lagenodifflugia vas*

Lake bottom sediment wind mixing probability

Calculated WMP for each sampled site was also included in the RDA analysis. The historic probability of winds strong enough to induce lake bottom sediment resuspension is termed the mixing probability. Hourly wind speed data was used to calculate the mixing probability. Data within the interval between 1953 and 2015 was obtained from the Fredericton INTL A climatological station (FIACS; 45° 52′ 08.000″ N, 66° 32′ 14.000″), which is located 40 km to the east-northeast (68° bearing). Additionally, data from December to April was excluded due to ice coverage on Harvey Lake during these months. This exclusion precludes any winds influence on the lake water column (Patterson et al., 2020). Using the Pandas Glob and Os modules of the Python computer programming language (version 3.7.4), individual CSV files were merged into a single data set based on each file representing a month of hourly logged meteorological data. According to the BWS, in order to generate the frequency, cumulative sum and percentage of occurrence, the Python, the Pandas, and Numpy modules were used to bin the hourly data by wind speed (km/h).

Results

Spearman rank correlation

The Spearman's correlation results (Fig. 2) revealed a strong positive correlation between water depth and *D. glans* (Ehrenberg, 1832) strain "glans" (0.60, *P*-value = < 0.0002). EM2 also correlated positively with *D. glans* "glans" (0.70, *P*-value = < 0.000007). Additionally, WMP had notable positive correlations with both faunal diversity (*H* or SDI; 0.60, *P*-value = < 0.0002) and the distribution of *Centropyxis discoides* Penard 1902 (0.60, *P*-value = < 0.0000002). There were also some negative correlations between WMP and arcellinidan taxa including *D. glans* strain "glans" (− 0.66, *P*-value = < 0.00003) and *C. discoides* (− 0.63, *P*-value = < 0.00008). Finally, EM2 correlated negatively with diversity (*H* or SDI; − 0.61, *P*-value = < 0.0001).

There are four variables of interest which include arsenic, mixing probability, water depth, and EM2. Arsenic contamination in Harvey Lake has been a concerning issue from the Harvey community. Mixing probability is linked to the impact of Arthur as it shows the areas that are likely to be impacted compared to ones which are not. Depth is an important control on arcellinidan distribution that can be linked to the wave base depth associated with Hurricane Arthur. EM2 is a resuspension of sediment particles associated with the impact of Arthur.

Cluster analysis

Results of the Q-mode cluster analysis and PVClust (Appendix 3—Supplementary Material) revealed four distinct arcellinidan assemblages: (1) Deep Water Reworking Assemblage (DWR; approximately unbiased probability value (AU *P*-value) = 89%; *n* = 16); (2) Arsenic Impact Assemblage (AI; AU *P-value* = 66%; *n* = 7); (3) Northern Shallow Water Assemblage A (NSWA; AU *P*-value = 92%; *n* = 5); and, (4) Northern Shallow Water Assemblage B (NSWB; AU *P*-value = 0%; *n* = 5). The R-mode cluster dendrogram revealed that the arcellinidan composition of the identified assemblages is mostly impacted by four taxa: (1) *Difflugia oblonga* (Ehrenberg 1832) strain "oblonga"; (2) *Difflugia elegans* (Penard 1890); (3) *D. glans* "glans"; (4) *D. glans* (Dujardin 1837) strain "magna".

Non-metric multidimensional scaling

Similar to the cluster analysis results, the NMDS biplot delineates four Arcellinida assemblages (Fig. 4). Assemblage NSWA and Assemblage NSWB overlap with each other (Fig. 4). Both of these assemblages are located in the northern section of Harvey Lake. The two main overlaps between assemblages NSWA and NSWB are Site 2 and 64. Samples of assemblage DWR clusters closer to the following taxa: *D. glans* "glans," *D. oblanga* "oblanga," *D. glans* "magna," *Difflugia bidens* Penard 1902, and *D. elegans*. Assemblage AI clusters closely to the following species: *Pontigulasia compressa* (Carter 1864) and *Lesquereusia spiralis* (Ehrenberg 1840). Assemblage NSWA clusters with following strains: *C. constricta* "constricta," *L. vas* and *D. acuminata*. Assemblage NSWB clusters with the following taxa: *C. aculeata* "aculeata," *C. aculeata* "discoides," *C. constricta* "aerophila," *C. constricta* "constricta," *D. curvicaulis*, and *L. spiralis*.

Redundancy analysis

Results of the RDA agree with the findings of cluster analysis and NMDS and reveals the same four arcellinidan assemblages (Fig. 5). Variance partitioning results show the first two RDA axes to be the most significant; together they explain 20.02% (*P*-value = 0.001) and 6.17% (*P*-value = 0.031) of the total Arcellinida variance, respectively. Of the 13 analyzed parameters, four explain 20.2% of the total variance in the arcellinidan distribution (WMP, EM2, arsenic concentration, and water depth; Fig. 5), with As being the most statistically significant of the four parameters (variance explained = 4.3%; *P*-value = 0.004; Appendix 4)—Supplementary Material. Arsenic is closely followed by WMP (variance explained = 3.1%; *P*-value = 0.009) and water depth (variance explained = 1%; *P*-value = 0.185).

Arcellinida assemblages

Deep Water Reworking Assemblage (DWR1; n = 16)

Assemblage DWR was mostly located in sites within the middle to southern section of Harvey

Lake (Fig. 1B). This assemblage occurs in 16 samples collected from the deepest sites, with a median water depth of 6.5 m (4.5–11.6 m) in silt-dominated substrates (median silt = 80%) with a relatively elevated proportion of sand (median sand% = 14.6%). Samples of DWR were characterized by a low mixing probability of (median = 17.65%; range = 0–63%) and elevated EM2 percentages (median = 82%; range = 0–94%) (Figs. 6, 7). The median SDI values for DWR are 2.4 (range 2.2–2.6, median SDI = 2.4).

The faunal composition of DWR was dominated by *D. oblonga* strain "oblonga" (median relative abundance = 20.93%; range = 14.3–32%) and *D. elegans* (median relative abundance = 17.58%; = 8.2–28.7%). Other species like *D. glans strain* "glans" had (median relative abundance = 12%; range = 4–19.4%) and *D. glans* strain "magna" had (median relative abundance = 9.02%; range = 3.6–16.1%).

Results of cluster analysis, NMDS, and RDA demonstrated that samples containing DWR closely clustered together (Figs. 3, 4, 5). Additionally, the RDA tri-plot showed that DWR associated positively with As, water depth, and EM2, and negatively with WMP (Fig. 5).

Arsenic Impact Assemblage (AI; n = 7)

Assemblage AI occurs mainly in samples collected from the southern area of Harvey Lake (Fig. 1B). This assemblage was found at water depths ranging from 3 to 6.6 m (median relative abundance = 5.5 m) with sample 61 being an outlier (depth = 3 m). Excluding sample 61, the water depth range for AI is 5.1–6.6 m.

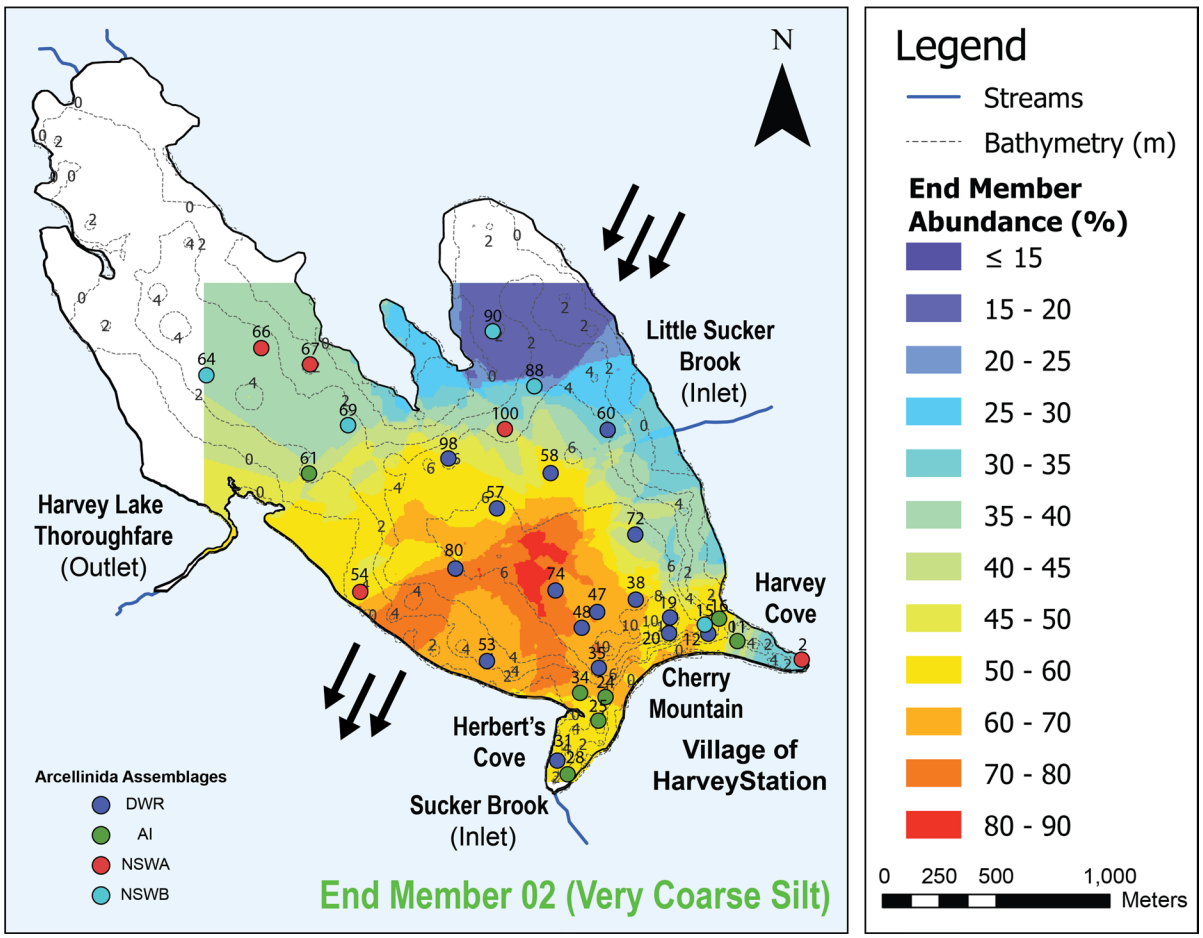

Fig. 6 Map of Harvey Lake with end member mixing analysis abundance (%). Red and orange areas are high abundant areas (70–90%). Purple and teal are low abundant areas (0–20%). Modified after Patterson et al. (2020)

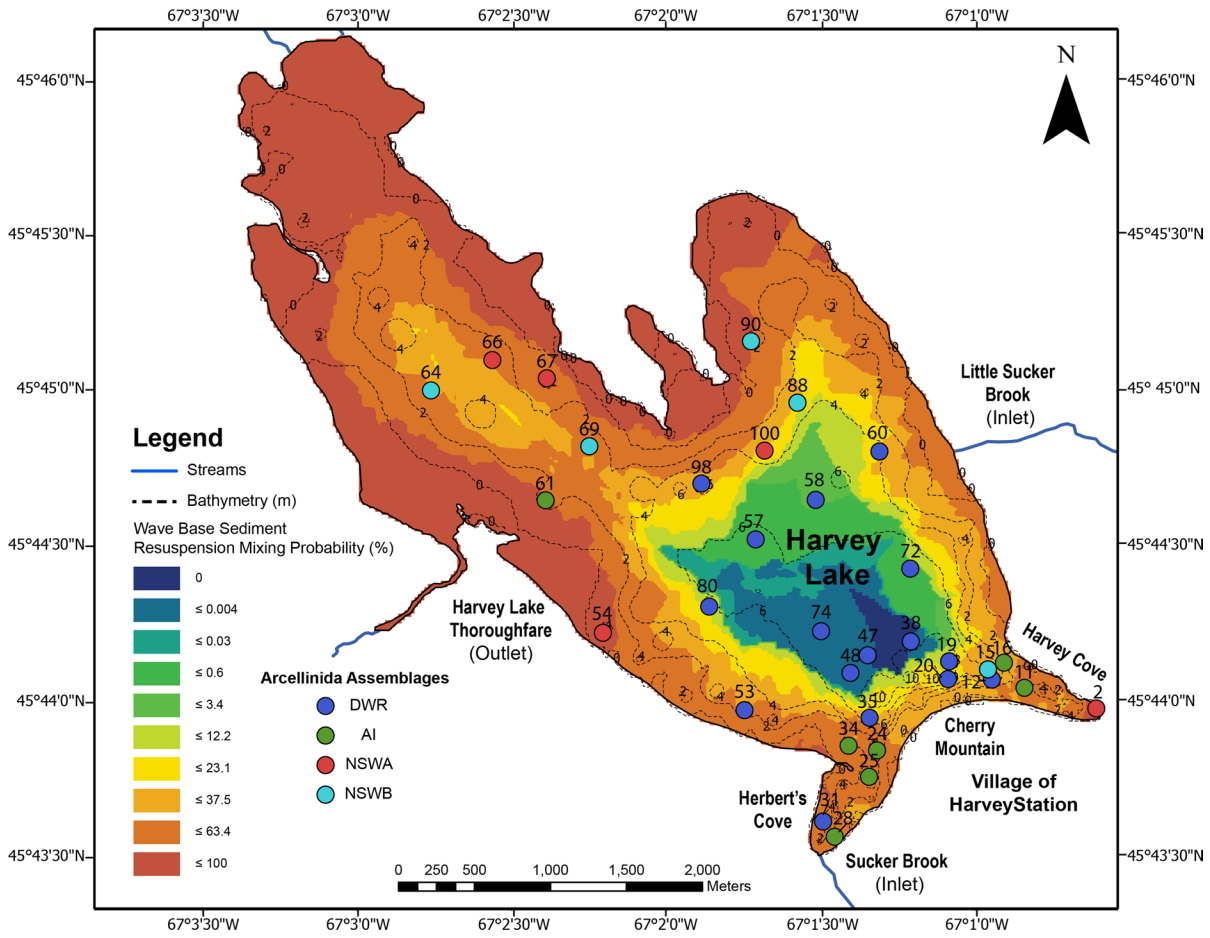

Fig. 7 Map of Harvey Lake with wave base sediment resuspension mixing probability (%). Red and orange areas are high mixing probability areas (63.5–100%). Dark blue and teal are low wind mixing probability areas (0–0.004%). Modified after Patterson et al. (2020)

AI was characterized by silt-dominated substrates (median relative abundance silt = 79%) with a similar proportion of sand as observed in DWR (median relative abundance sand% = 14.1%). Samples that comprise AI were characterized by a low WMP (median relative abundance = 37.5%; range = 37.5–100%) and a high EM2 proportions (median relative abundance = 63%; range = 0–82%, Figs. 6, 7). The SDI values for AI range between 2.58 and 2.71, with a median of 2.67.

Surface-sediment samples containing AI are clustered together (Figs. 3, 4, 5). The RDA tri-plot showed that samples of AI closely associated with As, and plotting away from WMP (Fig. 5). However, there were a few outlying samples within AI (11, 16, and 24) that were positively associated with WMP.

Assemblage AI was dominated by *D. oblonga* "oblonga" (16%; 9–17.5%) and *D. elegans* (15.5%; 9–19%). However, these taxa are present in lower proportions compared to in the DWR samples. Other taxa such as *D. glans* strain "glans" (10%; 7–13%) and *D. glans* strain "magna" (6.62%; 3.5–9.1%) were also present.

Northern Shallow Water Assemblage A (NSWA; n = 5)

Samples comprising NSWA occur in samples collected from the northern section of Harvey Lake (Fig. 1B). was Assemblage NSWA occurs in second most shallow sites (median relative abundance = 4.3 m; range of 3.5–4.6 m). This assemblage

inhabited silt-dominated substrates (median silt = 68%) with elevated presence of sand (median relative abundance sand% = 27%) that is higher than the levels in the DWR and AI samples. Samples of NSWA are characterized by a high WMP (median relative abundance = 63.4%; range = 23.1–100%) and a relatively low proportion of EM2 compared to that found in sites hosting DWR and AI (median relative abundance = 37%; range = 0–61%, Figs. 6, 7). The SDI values for NSWA range between 2.41 and 2.69 (median = 2.58).

Samples that comprise NSWA cluster together (Figs. 3, 4, 5). The RDA tri-plot showed that NSWA associated positively with WMP, and negatively with As and, to a lesser extent, EM2 and depth (Fig. 5).

Assemblage NSWA was dominated by *D. elegans* (17.4%; 9.2–19%) and *D. oblonga* strain "oblonga" (17.1%; 12.2–24%). Other species like *Lagenodiffflugia vas* (Leidy, 1874) (8.2%; 6.5–11.3%), *C. constricta* (Ehrenberg 1843) strain "constricta" (7.8%; 3.5–9.2%) and *D. glans* strain "magna" (5.5%; 3.2–6.7%) were also present in notable proportions. Although NSWA is still dominated by *D. elegans* and *D. oblonga* strain "oblonga," the percentages were smaller compared to DWR and AI (Fig. 8).

Northern Shallow Water Assemblage B (NSWB; n = 5)

Samples of NSWB were mostly located in the northern section of Harvey Lake (Fig. 1B). This assemblage was found in the shallowest sites with a water depth ranging from 2.8 to 7 m with a median relative water depth of 3.5 m. The 7 m depth was the outlier (range excluding sample 15 with 7 m depth = 2.8–3.8 m). Assemblage NSWB is characterized by silt-dominated substrates (median relative abundance silt = 69%) with slightly lower proportions of sand relative to NSWA (median relative abundance sand% = 20.5%). Samples of NSWB were characterized by a high WMP (range = 37.5%; range 37.5–63.4%) and relatively low EM2 content (median relative abundance = 44%; range = 0–84%, Figs. 6, 7). The SDI values for NSWB range between 2.5 and 2.8 (median relative abundance = 2.6).

Results of the cluster analysis, NMDS, and RDA demonstrated that samples containing NSWB closely clustered together (Figs. 3, 4, 5). The RDA tri-plot showed that NSWB associated positively with mixing probability, and negatively with arsenic.

Assemblage NSWB was dominated by *D. oblonga* strain "oblonga" (17.4%; 9.2–19%). *Difflugia glans* strain "glans" (8.2%; 6.5–11.3%), *D. glans* strain "magna" (7.8%; 3.5–9.2%), and *D. elegans* (5.5%; 3.2–6.7%), although present in elevated numbers, were less than observed in samples hosting DWR, AI, and NSWA.

Discussion

Arsenic

Of the four controlling variables considered, As explained the highest proportion of total variance in the Arcellinida distribution (4.28%; *P*-value = 0.004; Fig. 5). Several previous studies have shown that elevated levels of As adversely impact the spatial (e.g., Patterson et al., 1996; Reinhardt et al., 1998a, b; Nasser et al., 2016, 2020a, b; Riou et al., 2021) and temporal (Gavel et al., 2018) distribution of Arcellinida. These studies have consistently shown a faunal gradient from the presence of stressed arcellinidan assemblages where As levels are high to healthier environment indicator assemblages thriving in sites with lower As levels. The Arcellinida in Harvey Lake fall in the latter category as they were only modestly impacted by As concentrations in the lake substrate, with all assemblages being moderately (DWR; median SDI = 2.44; range = 2.24–2.56) to highly diverse (AI; median SDI = 2.67; range = 2.57–2.71, NSWA; median SDI = 2.58; range = 2.41–2.69, NSWB; median SDI = 2.59; range = 2.56–2.78) and showing no significant signs of stress in their faunal composition (e.g., high proportions of stress indicator taxa such as centropyxids; Nasser et al., 2016, 2020a, b; Riou et al., 2021; Fig. 2, Appendices 5, 6, 7, 8—Supplementary Material). The modest impact of As on the arcellinidan distribution is corroborated by the relatively low As concentrations measured throughout the Harvey Lake Basin (median As = 34.15 mg/kg; As range = 8.9–34.15 mg/kg), that are only slightly higher than the Interim Sediment Quality Guidelines (ISQG = 5.9 mg/kg) and Probable Effect Level (PEL = 17 mg/kg; CCME, 2002).

The intra-lake distribution of As showed a distinct spatial trend. Samples located adjacent to Cherry

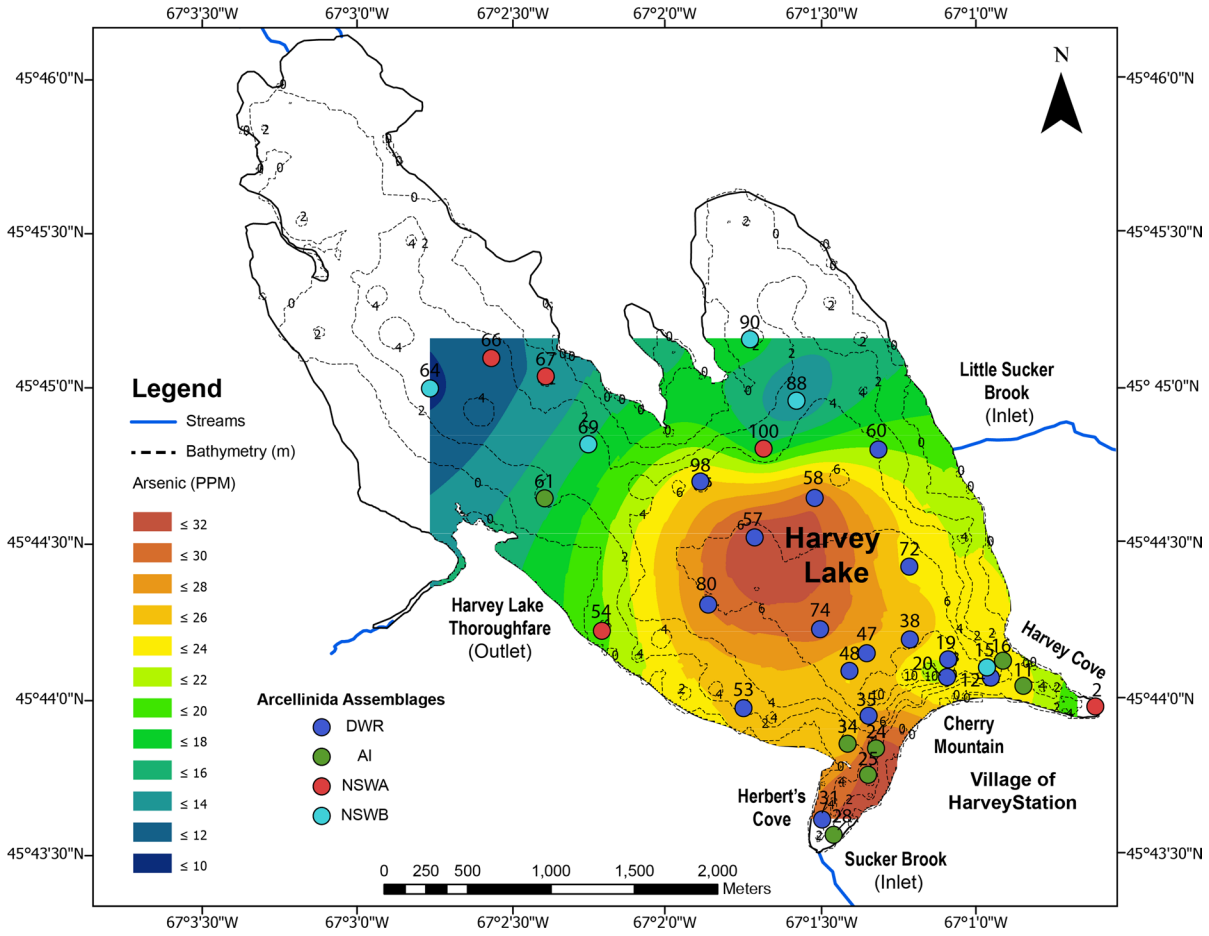

Fig. 8 Map of Harvey Lake with arsenic levels (ppm). Red and orange areas are high arsenic values (26–32+ ppm). Blue and green are low arsenic values (10–24 ppm) Modified after Patterson et al. (2020)

Mountain in the central and southern areas of Harvey Lake are characterized by slightly higher sedimentary As concentrations compared to more northern sites (Fig. 8; Appendices 5, 6, 7, and 8—Supplementary Material). Cherry Mountain is comprised of rhyolitic volcanic rocks where fluorite is an important constituent (Dostál et al., 2016). This rock-type rocks has previously been observed to contain As (Onishi and Sandell, 1954; Rango et al., 2013; Morales et al., 2015; McGrory et al., 2017). Therefore, sediment erosion from Cherry Mountain is a likely source of As to Harvey Lake. Elevated levels of As is a known issue reported by the community of Harvey. Of 108 well-water samples analyzed by the province of NB in 2008, 41 were found to contain of As concentration above Canadian drinking water levels of 10 µg/l (CBC, 2008). Elevated concentrations of As seem to be restricted to the sediment substrate in the lake though as regular water column monitoring carried out in Harvey Lake from 1999 to 2020 has consistently returned negligible As concentrations (New Brunswick Department of Environment and Local Government Lake Water Quality Data, 2020).

Variables influencing Arcellinida intra-lake distribution

Interpretation of the two-way cluster analysis dendrogram, supported by the PVClust and NMDS results, led to the identification of four Arcellinida assemblages (Figs. 2, 4). The results of the RDA and partial-RDA show that the faunal structure of the identified assemblages was controlled by four variables (As, WMP, water depth, and EM2) that

together explained 20.26% of the total variance in the intra-lake distribution of Arcellinida (Fig. 5). While the explained variance by these variables was relatively low, they explained the highest total variance of any combination of four variables, and explained only slightly less than an RDA model that included all 13 variables (23.45%). The selected variables, particularly the WMP and EM2 data, provide valuable corroborative evidence of a direct impact of storm-induced sediment re-suspension on the intra-lake spatial distribution of Arcellinida.

Wind mixing probability

WMP explained 3.1% of the total variance in the intra-lake Arcellinida distribution (Fig. 5). Several previous studies have shown that storms impact the diversity of macro- and micro-organism communities in lacustrine settings (e.g., Hughes et al., 2009; Harris et al., 2011). In Harvey Lake the RDA tri-plot showed WMP as plotting particularly close to NSWA and NSWB, which were primarily found within the water depths less than storm wave base (mostly < 4.4 m). Median SDI (2.56; range = 2.24–2.78) for the Harvey Lake Arcellinida assemblages reflects high faunal diversity, which may at least be partially attributable to storm-induced sediment re-suspension. In contrast, the negative association between WMP and assemblages DWR and AI may suggest a weak to no influence on assemblages that are found in substrates below the storm wave base. More work needs to be done to explore the link between mixing probability and Arcellinida distribution since we do not have any record of Arcellinida spatial distribution in the year before Arthur. A possible solution is to assess down core Arcellinida variability to see if Arthur impacted them.

EM2

EM2 explained 0.91% of the observed arcellinidan distributional variance (Fig. 5). Patterson et al. (2020) identified this very coarse silt (mode = 40 µm) particle size EM in Harvey Lake at all water depths, which was determined to be derived from sediment resuspension, mobilization, and deposition that resulted from a high wind driven deepening of the storm wave base associated with the passage of Post-Tropical Storm Arthur. The highest proportion of EM2 was observed in sites located in the western and southern sections of the lake. This distribution of EM2 is attributable to the impact of the counterclockwise wind field of Arthur (strong winds out of the NE), which led to the displacement of a significant portion of suspended sediments that eventually settled out of the water column in the western and southern parts of the lake. This assessment is further confirmed by the strong association between EM2 and assemblages DWR and AI. EM2 has a negative but non-significant association with WMP ($rs = -0.5$; P-value = 0.12; $n = 33$), which further supports the idea that EM2 has been resuspended, transported, and displaced from shallower to deeper parts of the lake during the passage of Post-Tropical Storm Arthur.

Water depth

Water depth explains 2.92% of the total variance in arcellinidan intra-lake distribution (Fig. 5). Several previous studies have shown water depth to have either a direct, due to thermal of chemical stratification (Tsyganov et al., 2019; Cockburn et al., 2020), or indirect impact on the distribution of Arcellinida (i.e., through impacting other lake parameters; Patterson et al., 1985, 1996; Payne, 2011). Although the water column in Harvey Lake was unstratified at the time of sampling, the RDA results show that arcellinidan assemblages DWR and AI display an association with water depth (Fig. 5). Such association was not surprising as both assemblages are from samples with similar water depth (of ~ 6.5 m). Both assemblages are characterized by higher relative abundances of *D. glans* strain "glans" (median *D. glans* strain "glans" = 9%) relative to NSWA and NSWB assemblages (median *D. glans* strain "glans" = 4.8%) that are comprised of samples collected in shallower water. *Difflugia glans* strain "glans" has been shown to be indicative of deeper water lacustrine substrates in several previous studies (Reinhardt et al., 1998a, b; Nasser et al., 2016; Cockburn et al., 2020). This relationship is also observed in the Harvey Lake samples by the close association between *D. glans* strain "glans" and water depth on the RDA tri-plot (Fig. 5) and a positive association between them ($rs = 0.6$; P-value = 0.0002, $n = 33$; Appendix 3—Supplementary Material).

Intra-lake Arcellinida response to storm sediment resuspension

The results of this study provide evidence of the impact of Post-Tropical Storm Arthur on the sediment and arcellinidan distribution throughout the Harvey Lake Basin. Sedimentologically, the mapping by Patterson et al. (2020) of the intra-lake distribution of the coarse silt fraction, EM2, its prevalence in deeper substrates, and its strong negative association with WMP led them to conclude that this EM originated from the resuspension of sediments by Arthur in areas of the lake at water depths shallower than the storm wave base depth of 4.4 m, and their displacement in the water column to all lake water depths. The distribution of EM2 in the SW part of the lake basin was the result of the high winds associated with the passage of Arthur coming out of the NE.

The arcellinidan distributional response to suspension into the water column by Arthur was subtle yet notable. The identified arcellinidan assemblages are highly diverse, which may be a result of homogenization related to storm sediment and entrained Arcellinida suspension and subsequent re-sedimentation throughout the lake basin. While the observed assemblages are similar in terms of their faunal structure, they are distinct enough to be divided into statistically significant assemblages, that provides insight into how Post-Tropical Storm Arthur impacted their composition. For example, the northern assemblages, NSWA and NSWB, are characterized by a weak statistical significance (AU P-value range = 0–66%), which suggests that the samples of the assemblages have a similar faunal structure. This is because these shallow water assemblages were likely more impacted by storm-induced wave base mixing of sediment. In contrast, the deeper water assemblages, DWR and AI, located in sediment beyond the direct impact of storm wave base reworking, have a significantly higher level of faunal structure consistency (AU P-value range = 89–92%), with the addition storm-derived shallower water assemblage over printing.

Conclusion

This project was carried out to assess the impact of Post-Tropical Storm Arthur (2014) and other variables on the distribution of Arcellinida taxa and assemblages throughout the Harvey Lake, New Brunswick Basin. An assessment of arcellinidan response to this large storm provides insight on the general impact of large storms on lake ecosystems as this group of shelled amoebae comprise an important intermediary component within aquatic food chains, and as such are sensitive bioindicators of environmental change.

Harvey Lake is characterized by four distinct Arcellinida assemblages (1–4). Assemblages NSWA and NSWB occur in samples located in the northern part of the lake, and DWR and AI are found in samples collected from deeper water areas in southern sections of the lake. The RDA and partial-RDA analyses resulted in the identification of four key variables that collectively explained 20.2% of the variance in the Arcellinida distribution; WMP, EM2 (coarse silt), water depth, and As. The most significant influence on the distribution of arcellinidan taxa and assemblages throughout the Harvey Lake Basin was driven by sedimentary As concentration, whereby As was likely derived from volcanic bedrock in the catchment, with concentrations slightly exceeding the Canadian Council of Ministers of the Environments ISQG of 5.9 mg/kg and PEL for the Protection of Aquatic Life of 17 mg/kg. Substrate and associated entrained Arcellinida tests that were suspended into the water column due to a deepening of the wave base during the passage of Post-Tropical Storm Arthur also had a significant influence on the distribution of arcellinidans taxa and assemblages. In deeper water in the southern part of the lake, below storm wave base, the diverse arcellinidan assemblages were comprised of in situ (e.g., *D. glans* "glans"), as well as allochthonous taxa, that had been suspended into the water column in shallower parts of the lake and subsequently redeposited throughout the entire lake basin at all water depths. These results indicate that sediment suspension and re-deposition, particularly in shallower areas of lakes, is a sampling design parameter that needs to be considered, particularly in areas that may be influenced by periodic great storms.

Acknowledgements We thank Jochen Schroer of NATECH Environmental Services for providing a shapefile for the Baseline Bathymetry Map. We also acknowledge the contributions of Dr. Sheryl Bartlett, Chairperson New Brunswick Alliance of Lake Associations and Past Chairperson of the Harvey Lake Association for facilitating the research on Harvey Lake. We thank Roy T. Patterson for contributing his time and a boat for

sample collection and to Zacchaeus Compson, University of New Brunswick, for aiding in the field collection of samples. We acknowledge the very helpful comments and data checking provided by the anonymous reviewers that significantly improved the manuscript.

Funding This work was supported by NSERC Discovery (#RGPIN05329) and NRCan Clean Technology (#CGP-17-0704) Grants to RTP.

Data availability The datasets used in this study are available at reasonable request from the corresponding author.

Declarations

Conflict of interest The authors declare that they have no known competing financial interests or personal relationships that could have appeared to influence the work reported in this paper.

References

Alley, R. B., J. Marotzke, W. D. Nordhaus, J. T. Overpeck, D. M. Peteet, R. A. Pielke Jr., R. T. Pierrehumbert, P. B. Rhines, T. F. Stocker, L. D. Talley & J. M. Wallace, 2003. Abrupt climate change. Science 299: 2005–2010.

Bailey, W. G., W. G. Bailey, T. R. Oke & W. R. Rouse, 1997. Surface climates of Canada, Vol. 4. McGill-Queen's Press-MQUP, Montreal:

Canadian Council of Ministers of the Environment (CCME), 2002. Canadian Sediment Quality Guidelines for the Protection of Aquatic Life. In: Canadian Environment Quality Guidelines.

CBC, 2008. Harvey Looks at Options to Deal with Uranium, Arsenic in Water. CBC New Brunswick [available on internet at https://www.cbc.ca/news/canada/new-brunswick/harvey-looks-at-options-to-deal-with-uranium-arsenic-in-water-1.741216]. Accessed 23 March 2021.

Charman, D. J., D. Hendon, W. A. Woodland & Quaternary Research Association, 2000. The Identification of Testate Amoebae (Protozoa: Rhizopoda) in Peats. Quaternary Research Association.

Cockburn, N., J. Corsaut, M. S. Kovacs, K. St Lawrence & J. W. Hicks, 2020. Validation protocol for current good manufacturing practices production of [^{15}O] water for hybrid PET/MR studies. Nuclear Medicine Communications 41: 1100–1105.

Dietze, E., K. Hartmann, B. Diekmann, J. IJmker, F. Lehmkuhl, S. Opitz, G. Stauch, B. Wünnemann & A. Borchers, 2012. An end-member algorithm for deciphering modern detrital processes from lake sediments of Lake Donggi Cona, NE Tibetan Plateau, China. Sedimentary Geology 243: 169–180.

Dostál, J., J. Pšenčík, & D. Zigmantas, 2016. In situ mapping of the energy flow through the entire photosynthetic apparatus. Nature Chemistry 8(7): 705–710.

Eden, D. N. & M. J. Page, 1998. Palaeoclimatic implications of a storm erosion record from Late Holocene lake sediments, North Island, New Zealand. Palaeogeography, Palaeoclimatology, Palaeoecology 139: 37–58.

Engle, V. D., J. L. Hyland & C. Cooksey, 2009. Effects of Hurricane Katrina on benthic macroinvertebrate communities along the northern Gulf of Mexico coast. Environmental Monitoring and Assessment 150: 193–209.

Fishbein, E. & R. T. Patterson, 1993. Error-weighted maximum likelihood (EWML): a new statistically based method to cluster quantitative micropaleontological data. Journal of Paleontology 67: 475–486.

Gallagher, E., H. Wadman, J. McNinch, A. Reniers & M. Koktas, 2016. A conceptual model for spatial grain size variability on the surface of and within beaches. Journal of Marine Science and Engineering 4: 38.

Gavel, P. K., D. Dev, H. S. Parmar, S. Bhasin & A. K. Das, 2018. Investigations of peptide-based biocompatible injectable shape-memory hydrogels: differential biological effects on bacterial and human blood cells. ACS Applied Materials and Interfaces 10: 10729–10740.

Gregory, B. R., R. T. Patterson, E. G. Reinhardt, J. M. Galloway & H. M. Roe, 2019. An evaluation of methodologies for calibrating Itrax X-ray fluorescence counts with ICP-MS concentration data for discrete sediment samples. Chemical Geology 521: 12–27.

Haarsma, R. J., J. F. Mitchell & C. A. Senior, 1993. Tropical disturbances in a GCM. Climate Dynamics 8: 247–257.

Harris, F., S. R. Dennison & D. A. Phoenix, 2011. Anionic antimicrobial peptides from eukaryotic organisms and their mechanisms of action. Current Chemical Biology 5: 142–153.

Hughes, S. J., J. M. Santos, M. T. Ferreira, R. Caraca & A. M. Mendes, 2009. Ecological assessment of an intermittent Mediterranean river using community structure and function: evaluating the role of different organism groups. Freshwater Biology 54: 2383–2400.

Jensen, R. E., M. A. Cialone, R. S. Chapman, B. A. Ebersole, M. Anderson & L. Thomas, 2012. Lake Michigan Storm: Wave and Water Level Modeling. Engineer Research and Development Center Vicksburg MS Coastal and Hydraulics Lab.

Kihlman, S. & T. Kauppila, 2012. Effects of mining on testate amoebae in a Finnish lake. Journal of Paleolimnology 47: 1–15.

Kruskal, J. B., 1964. Non-metric multidimensional scaling: a numerical method. Psychometrika 29: 115129.

Legendre, P. & E. D. Gallagher, 2001. Ecologically meaningful transformations for ordination of species data. Oecologia 129: 271–280.

Macumber, A. L., R. T. Patterson, J. M. Galloway, H. Falck & G. T. Swindles, 2018. Reconstruction of Holocene hydroclimatic variability in subarctic treeline lakes using lake sediment grain-size end-members. The Holocene 28: 845–857.

Magurran, A. E., 1988. Ecological Diversity and Its Measurement, Princeton University Press, Princeton:

Maintainer, K. & R. Kolde, 2019. Package "pheatmap" Type Package Title Pretty Heatmaps.

McGrory, E. R., C. Brown, N. Bargary, N. H. Williams, A. Mannix, C. Zhang, T. Henry, E. Daly, S. Nicholas, B. M. Petrunic & M. Lee, 2017. Arsenic contamination of drinking water in Ireland: a spatial analysis of occurrence

and potential risk. Science of the Total Environment 579: 863–1875.
McKerrow, W. S. & A. M. Ziegler, 1971. The Lower Silurian paleogeography of New Brunswick and adjacent areas. The Journal of Geology 79: 635–646.
Medioli, F. S. & D. B. Scott, 1983. Holocene Arcellacea (Thecamoebians) from Eastern Canada (No. 21), Cushman Foundation for Foraminiferal Research, Ithaca:
Miller, K. B., C. E. Brett & K. M. Parsons, 1988. The paleoecologic significance of storm-generated disturbance within a Middle Devonian muddy epeiric sea. Palaios 3(1): 35–52.
Mitchell, J. F. B., S. Manabe, T. Tokioka & V. Meleshko, 1990. Equilibrium climate change and its implications for the future. Climate Change: The IPCC Scientific Assessment 131: 172.
Morales, N. A., D. Martínez, J. V. García-Meza, I. Labastida, M. A. Armienta, I. Razo & R. H. Lara, 2015. Total and bioaccessible arsenic and lead in soils impacted by mining exploitation of Fe-oxide-rich ore deposit at Cerro de Mercado, Durango, Mexico. Environmental Earth Sciences 73: 3249–3261.
Murray, M. R., 2002. Is laser particle size determination possible for carbonate-rich lake sediments? Journal of Paleolimnology 27: 173–183.
Nasser, N. A. & R. T. Patterson, 2015. Conicocassis, a new genus ofArcellinina (testate lobose amoebae). Palaeontologia Electronica 18(46A): 1–11.
Nasser, N. A., R. T. Patterson, H. M. Roe, J. M. Galloway, H. Falck, M. J. Palmer, C. Spence, H. Sanei, A. L. Macumber & L. A. Neville, 2016. Lacustrine Arcellinina (testate amoebae) as bioindicators of arsenic contamination. Microbial Ecology 72: 130–149.
Nasser, N. A., R. T. Patterson, H. M. Roe, J. M. Galloway, H. Falck & H. Sanei, 2020a. Use of Arcellinida (testate lobose amoebae) arsenic tolerance limits as a novel tool for biomonitoring arsenic contamination in lakes. Ecological Indicators 113: 106177.
Nasser, N. A., R. T. Patterson, J. M. Galloway & H. Falck, 2020b. Intra-lake response of Arcellinida (testate lobose amoebae) to gold mining-derived arsenic contamination in northern Canada: Implications for environmental monitoring. Peer J 8: e9054.
New Brunswick Department of Environment and Local Government Lake Water Quality Data, 2020. Chart for Arsenic [available on internet at https://www.elgegl.gnb.ca/LakesNB-NBLacs/en/Sample/LocationResultChart?id=29]. Accessed 1 Feb 2021.
Ogden, G. G. & R. H. Hedley, 1980. An atlas of freshwater testate amoebae. Soil Science 130: 176.
Oliva, F., A. E. Viau, M. C. Peros & M. Bouchard, 2018. Paleotempestology database for the western North Atlantic Basin. The Holocene 28: 1664–1671.
Onishi, H. & E. B. Sandell, 1954. Photometric determination of traces of antimony with Rhodamine B after sulfide precipitation. Analytica Chimica Acta 11: 44–450.
Pachauri, R. K., M. R. Allen, V. R. Barros, J. Broome, W. Cramer, R. Christ, J. A. Church, L Clarke, Q. Dahe, P. Dasgupta & N. K. Dubash, 2014. Climate Change 2014: Synthesis Report. Contribution of Working Groups I, II and III to the Fifth Assessment Report of the Intergovernmental Panel on Climate Change: 151.
Pajari, G. E. & N. Rast, 1973. The Harvey volcanic area. In Geology of New Brunswick, Field Guide to Excursions, New England Intercollegiate Geological Conference, Department of Geology, University of New Brunswick, Fredericton, New Brunswick, Trip A-14 and B-11: 119–123.
Patterson, R. T. & E. Fishbein, 1989. Re-examination of the statistical methods used to determine the number of point counts needed for micropaleontological quantitative research. Journal of Paleontology 63: 245–248.
Patterson, R. T. & A. Kumar, 2002. A review of current testate rhizopod (thecamoebian) research in Canada. Palaeogeography, Palaeoclimatology, Palaeoecology 180: 225–251.
Patterson, R. T., K. D. MacKinnon, D. B. Scott & F. S. Medioli, 1985. Arcellaceans ("thecamoebians") in small lakes of New Brunswick and Nova Scotia; modern distribution and Holocene stratigraphic changes. The Journal of Foraminiferal Research 15: 114–137.
Patterson, R. T., T. Baker & S. M. Burbidge, 1996. Arcellaceans (thecamoebians) as proxies of arsenic and mercury contamination in northeastern Ontario lakes. The Journal of Foraminiferal Research 26: 172–183.
Patterson, R. T., E. D. Lamoureux, L. A. Neville & A. L. Macumber, 2013. Arcellacea (testate lobose amoebae) as pH indicators in a pyrite mine-acidified lake, Northeastern Ontario, Canada. Microbial Ecology 65: 541–554.
Patterson, R. T., V. Mazzella, A. L. Macumber, B. R. Gregory, C. W. Patterson, N. A. Nasser, H. M. Roe, J. M. Galloway & E. G. Reinhardt, 2020. A novel protocol for mapping the spatial distribution of storm derived sediment in lakes. SN Applied Sciences 2: 1–16.
Payne, R. J., 2011. Can testate amoeba-based palaeohydrology be extended to fens? Journal of Quaternary Science 26: 15–27.
Peng, Y., J. Xiao, T. Nakamura, B. Liu & Y. Inouchi, 2005. Holocene East Asian monsoonal precipitation pattern revealed by grain-size distribution of core sediments of Daihai Lake in Inner Mongolia of north-central China. Earth and Planetary Science Letters 233: 467–479.
Pilarczyk, J. E., T. Dura, B. P. Horton, S. E. Engelhart, A. C. Kemp & Y. Sawai, 2014. Microfossils from coastal environments as indicators of paleo-earthquakes, tsunamis and storms. Palaeogeography, Palaeoclimatology, Palaeoecology 413: 144–157.
R core Team, 2014. R: A Language and Environment for Statistical Computing. http://www.R-project.org.
Rango, T., A. Vengosh, G. Dwyer & G. Bianchini, 2013. Mobilization of arsenic and other naturally occurring contaminants in groundwater of the Main Ethiopian Rift aquifers. Water Research 47: 5801–5818.
Rao, C. R., 1995. A Review of Canonical Coordinates and an Alternative to Correspondence Analysis Using Hellinger Distance. Qüestiió: quaderns d'estadística i investigació operativa.
Reinhardt, E. G., J. Blenkinsop & R. T. Patterson, 1998a. Assessment of a Sr isotope vital effect ($^{87}Sr/^{86}Sr$) in marine taxa from Lee Stocking Island, Bahamas. Geo-Marine Letters 18: 241–246.
Reinhardt, E. G., A. P. Dalby, A. Kumar & R. T. Patterson, 1998b. Arcellaceans as pollution indicators in mine tailing

contaminated lakes near Cobalt, Ontario, Canada. Micropaleontology 44: 131–148.
Riou, L., N. A. Nasser, R. T. Patterson, B. R. Gregory, J. M. Galloway & H. Falck, 2021. Lacustrine Arcellinida (testate lobose amoebae) as bioindicators of arsenic concentration within the Yellowknife City Gold Project, Northwest Territories, Canada. Limnologica 87: 125862.
Roe, H. M., R. T. Patterson & G. T. Swindles, 2010. Controls on the contemporary distribution of lake thecamoebians (testate amoebae) within the Greater Toronto Area and their potential as water quality indicators. Journal of Paleolimnology 43: 955–975.
Scott, D. B. & J. O. R. Hermelin, 1993. A device for precision splitting of micropaleontological samples in liquid suspension. Journal of Paleontology 67: 151–154.
Siemensma, F. J., 2019. Microworld, World of Amoeboid Organisms. World-Wide Electronic Publication, Kortenhoef.
Suzuki, R. & H. Shimodaira, 2006. Pvclust: an R package for assessing the uncertainty in hierarchical clustering. Bioinformatics 22(12): 1540–1542.
Taiyun, M. & T. Wei, 2016. Title Visualization of a Correlation Matrix.
Tsyganov, A. N., E. A. Malysheva, A. A. Zharov, T. V. Sapelko & Y. A. Mazei, 2019. Distribution of benthic testate amoeba assemblages along a water depth gradient in freshwater lakes of the Meshchera Lowlands, Russia, and utility of the microfossils for inferring past lake water level. Journal of Paleolimnology 62: 137–150.
Van Hengstum, P. J., E. G. Reinhardt, J. I. Boyce & C. Clark, 2007. Changing sedimentation patterns due to historical land-use change in Frenchman's Bay, Pickering, Canada: evidence from high-resolution textural analysis. Journal of Paleolimnology 37: 603–618.
Ward, J. H., Jr., 1963. Hierarchical grouping to optimize an objective function. Journal of the American Statistical Association 58: 236–244.
Webster, P. J., G. J. Holland, J. A. Curry & H. R. Chang, 2005. Changes in tropical cyclone number, duration, and intensity in a warming environment. Science 309: 1844–1846.
Weltje, G. J. & M. A. Prins, 2003. Muddled or mixed? Inferring palaeoclimate from size distributions of deep-sea clastics. Sedimentary Geology 162: 39–62.
Weltje, G. J. & M. A. Prins, 2007. Genetically meaningful decomposition of grain-size distributions. Sedimentary Geology 202: 409–424.
Weltje, G. J., M. R. Bloemsma, R. Tjallingii, D. Heslop, U. Röhl & I. W. Croudace, 2015. Prediction of geochemical composition from XRF core scanner data: a new multivariate approach including automatic selection of calibration samples and quantification of uncertainties. In Micro-XRF Studies of Sediment Cores. Springer, Dordrecht: 507–534.